AKADÉMIAI KIADÓ

UNIVERSITY of DEBRECEN

International Review of Applied Sciences and Engineering

DOI:
10.1556/1848.2021.00352

ORIGINAL RESEARCH PAPER

A relative degree one modified active disturbance rejection control for four-tank level control system

Zahraa Sabah Hashim[1] and Ibraheem Kasim Ibraheem[1,2]*

[1] Department of Electrical Engineering, College of Engineering, University of Baghdad, Al-Jadriyah, 10001, Baghdad, Iraq

[2] Department of Computer Engineering Techniques, Al-Rasheed University College, Baghdad, 10001, Iraq

Received: July 25, 2021 • Accepted: September 28, 2021

ABSTRACT

This paper deals with the disturbance rejection, parameter uncertainty cancelation, and the closed-loop stabilization of the water level of the four-tank nonlinear system. For the four-tank system with relative degree one, a new structure of the active disturbance rejection control (ADRC) has been presented by incorporating a tracking differentiator (TD) in the control unit to obtain the derivate of the tracking error. Thus, the nonlinear-PD control together with the TD serves as a new nonlinear state error feedback. Moreover, a sliding mode extended state observer is presented in the feedback loop to estimate the system's state and the total disturbance. The proposed scheme has been compared with several control schemes including linear and nonlinear versions of ADRC techniques. Finally, the simulation results show that the proposed scheme achieves excellent results in terms of disturbance elimination and output tracking as compared to other conventional schemes. It was able to control the water levels in the two lower tanks to their desired value and exhibits excellent performance in terms of Integral Time Absolute Error (ITAE) and Objective Performance Index (OPI).

KEYWORDS

four-tank system, Active Disturbance Rejection Control (ADRC), Integral Time Absolute Error (ITAE), Objective Performance Index (OPI), extended state observer, tracking differentiator, nonlinear state error feedback

1. INTRODUCTION

A Four-tank system is one of the most important industrial and chemical processes that contain several manipulated variables, strongly interacting, controlled variables, parameters uncertainties, and nonlinear dynamics. Therefore, due to all of these reasons, the need to find suitable multivariable control techniques increases over time. A Four-tank system is a laboratory process that was originally proposed by Karl Henrik Johansson [1–3]. It becomes one of the popular case studies that show various behaviors, one of these behaviors is the effect of multivariable zeros in both linear and nonlinear models.

The Four-tank system is a multi-input multi-output (MIMO) system and a good motivation to find a new technique to solve multivariable control problems. In the present time, many researchers show different control techniques to solve these problems. The main control techniques that are used with the four-tank system are Decoupled PI controller [4], Fuzzy-PID [5], second-order sliding mode control [6], IMC-based PID [7]. In [8], various control schemes are used such as gain scheduling controller, a linear parameter varying controller, and input-output feedback linearization. J-Han in [9] proposed a new technique to eliminate the disturbance and uncertainty for SISO and MIMO systems, this technique is called active disturbance rejection control. It consists of tracking differentiator (TD), an

*Corresponding author.
E-mail: ibraheemki@alrasheedcol.edu.iq

AKJournals

extended state observer (ESO), and nonlinear state error feedback. Each part of ADRC has a function to accomplish; TD provides a derivative to get fast tracking, ESO estimates and rejects the total disturbance which contains plant uncertainties, exogenous disturbances, and system dynamics. In [10], the authors demonstrated the stability of the ADRC for ball and beam system. The results showed an effective performance for both ADRC and ESO. In [11], the author reported the importance of choosing the bandwidth of the observer. A large value of observer bandwidth increases noise sensitivity, and a lower value slows down the estimation convergence. Therefore, it must be selected carefully. In [12], the author proposed a new configuration for the four-tank system, a new control strategy for a class of controllers such as PID, LADRC, and ADRC. This control strategy depends on tracking error to measure the controlled target. The experiment and simulation results examined an improvement in output tracking and disturbance suppression. The authors in [13, 14] proposed an improved version for the nonlinear ESO and nonlinear state error feedback control to reduce the chattering phenomena and actuator saturation. In [15], the authors introduced the model predictive control with the linear model of the four tanks system to stabilize and optimize the input and the output. Authors of [16] proposed an Adaptive Pole Placement Controller (APPC) and a robust Adaptive Sliding Mode Controller (ASMC) to improve the robustness and rapidity of various industrial processes such as the four tanks system. In [17], the authors proposed a decentralized model predictive controller with the nonlinear model of the four tanks system to ensure the bound of the linearizing error by converting the system into a class of subsystems which in turn was converted into an n-number of robust tubes. In [18], the author has introduced a controller design based on a neural network. Although all the above studies proposed an excellent and accurate controller for the four-tank system but still there two drawbacks in their work. Firstly, some of the above studies used the linearized model of the four-tank system except for [3, 6, 12, 17, 18]. As a result, the controller was incapable to follow the nonlinear dynamics of the system, especially in the practical implementation. Secondly, exogenous disturbance and parameter uncertainties were not taken into consideration. Motivated by the above studies, this paper considers parameter uncertainties and exogenous disturbances in the control design of the four-tank system. Moreover, a new nonlinear controller with a tracking differentiator was also used to control the nonlinear model of the four-tank system. This combination will form the proposed ADRC for the four-tank system with a unit relative degree that gives an excellent, smooth, and fast output response with reduced sensitivity to the noise due to the adoption of the TD with nonlinear PID (NLPID) controller. The contribution of this paper lies in the following. A new nonlinear controller has been proposed by integrating the nonlinear PID controller with the tracking differentiator (TD). The TD replaces the traditional differentiator needed in the derivative part of the PID control design; thus, a new nonlinear PID controller with less sensitivity to the measurement noise is obtained. This new nonlinear PID controller has been integrated with the sliding mode extended state observer (SMESO) to form an improved active disturbance rejection control. Moreover, the genetic algorithm has been used to tune the parameters. A new performance index has been proposed to tune the parameters of the proposed nonlinear PID controller and the SMESO. A new multi-objective performance index is used in the minimization process, which includes the integral time absolute error, the absolute of the control signals, and the square of the control signals for both channels.

The rest of the paper is organized as follows: Section 2 presents the modeling of the four-tank system. Section 3 presents the proposed ADRC with a unit relative degree system. Section 4 presents the convergence of SMESO. Section 5 illustrates simulation results and discussion of the results, finally section 6 presents the conclusion of the work.

2. MODELING OF THE FOUR-TANK SYSTEM

As shown in Fig. 1, the four-tank system consists of two pumps, a source tank, two valves, and four water tanks. ***Pump A*** extracts the water from the source tank and pours it into $tank_1$ *and* $tank_4$. Symmetrically, ***pump B*** extracts the water from the source tank and pours it into $tank_2$ *and* $tank_3$. Then the output flow of the pumps is divided into two by using three-way valves. ***Valve*1** separated the spilled water into $tank_1$ by a fraction γ_1 and to tank_4 by a fraction $(1 - \gamma_1)$. In the same way, $tank_2$ *and* $tank_3$ are fed from ***pump B***, and by ***Valve*2** the water distributed to tank_2 by a fraction γ_2 and to $tank_3$ by a fraction $(1 - \gamma_2)$. By gravity action, the liquid in tank_3 flows into $tank_1$ and then from $tank_1$ returns to the source tank. Symmetrically, the liquid in tank_4 flows into $tank_2$ and then returns to the source tank. The water level in tank_1 and $tank_2$ is controlled by the two pumps, the flow of the water to tank_1 is $\gamma_1 k_1 u_1$ and for $tank_4$ is $(1 - \gamma_1) k_1 u_1$, similarly for the flow of the water to $tank_2$ is $\gamma_2 k_2 u_2$ and for tank_3 is $(1 - \gamma_2) k_2 u_2$. In this paper, h_3 is considered as the internal dynamics of is h_1, symmetrically h_4 is the internal dynamics of h_2. So there are two disturbances, the first is the flow from the upper tank to the lower tank and the second one is the flow rate. The fraction (γ_1, γ_2) specifies the position of multivariable zeros which operate the system in minimum phase or non-minimum phase, in other words, these multivariable zero depend on

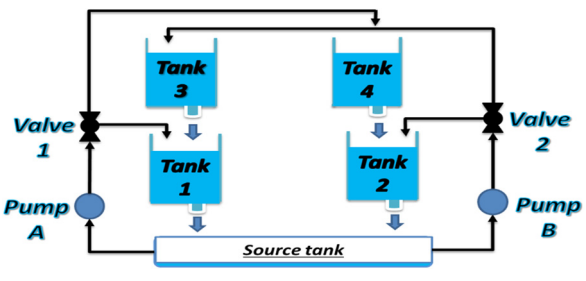

Fig. 1. Schematic diagram of the four-tank system

the position of valves, $1<\gamma_1+\gamma_2<2$ minimum phase and for non-minimum phase $0<\gamma_1+\gamma_2<1$. In this paper, the system operates in *minimum phase mode*. According to Bernoulli equation and Mass balance, the nonlinear model of the four-tank system is the following [1]:

$$\dot{h}_1 = -\frac{a_1}{A_1}\sqrt{2gh_1} + \frac{a_3}{A_1}\sqrt{2gh_3} + \frac{\gamma_1 k_1}{A_1}(u_1 + d_1) \quad (1)$$

$$\dot{h}_2 = -\frac{a_2}{A_2}\sqrt{2gh_2} + \frac{a_4}{A_2}\sqrt{2gh_4} + \frac{\gamma_2 k_2}{A_2}(u_2 + d_2) \quad (2)$$

$$\dot{h}_3 = -\frac{a_3}{A_3}\sqrt{2gh_3} + \frac{(1-\gamma_2)k_2}{A_3}u_2 \quad (3)$$

$$\dot{h}_4 = -\frac{a_4}{A_4}\sqrt{2gh_4} + \frac{(1-\gamma_1)k_1}{A_4}u_1 \quad (4)$$

$$y_1 = k_c h_1 \quad (5)$$

$$y_2 = k_c h_2 \quad (6)$$

where A_j the cross-sectional area of is $tank_j$, a_j is the cross-section area of the outlet hole, h_j is the water level in $tank_j$, $j = \{1,\ldots,4\}$. u_1 and u_2 are the voltages applied to ***pump A*** and ***pump B*** respectively, g is the acceleration of gravity and k_c is a calibrated constant, k_1 and k_2 are pump proportionality constants, k_1u_1 and k_2u_2 are the water flow rate generated by ***pump A*** *and* ***pump B*** respectively, d_1 and d_2 are the exogenous disturbances by the flow rate. We assume that the water flow generated by pump A and pump B is proportional to its applied voltages (u_1 and u_2).

3. PROPOSED ACTIVE DISTURBANCE REJECTION CONTROL WITH A UNIT RELATIVE DEGREE

J. Han [9], introduced an excellent method during the last decade to deal with the disturbances and uncertainties of the nonlinear system. This method is known as Active Disturbance Rejection Control (ADRC). The term active in ADRC means that ADRC estimates/cancels the total disturbance (parameter uncertainties, external disturbance, system dynamics, and any unknown or unwanted dynamics) in an online manner, which shows the effectiveness of ADRC. Generally, ADRC consists of three essential elements, tracking differentiator (TD), Nonlinear State Error Feedback controller (NLSEF), and the Extended State Observer (ESO).

In general, for a system with a unit relative degree or relative degree one ($\rho = 1$) there is no need to use tracking differentiator (TD) because the ESO estimates two states, z_1 is the system state and z_2 is the generalized disturbance. So, the TD is combined with the nonlinear state error feedback (NLSEF) controller to constitute a new control structure for the ADRC. The general form of the proposed ADRC with relative degree one is shown in Fig. 2 below. It is illustrated that instead of the reference signal $r(t)$, the error signal $\tilde{e}(t)$ is using as an input to TD to obtain a smooth signal of the error and its derivative which in turn is used in the NLSEF to get the required control output $u_0(t)$. Furthermore, ESO will convert the system into a chain of integrators by estimating and canceling the total disturbance in an online fashion. Finally, after connecting the circuit using Matlab/Simulink, GA is used as an optimization technique to find optimal and suitable values for the parameters of TD, NLSEFC, and ESO. The proposed ADRC consists of a TD, an NLSEF, and a nonlinear ESO (NLESO) and it is explained as follows.

3.1. Tracking differentiator (TD)

The use of a tracking differentiator has been increased in the last decade, to avoid set point jump, provide fast output tracking, and extract an accurate differentiated signal from the reference one that was not ideal in the classical (ordinary) differentiation [9, 19]. It is necessary to provide a transient profile to reduce the effect of peaking and chattering phenomena, achieving high control performance and high robustness against noise. The proposed method shows that it is not impossible to use TD with systems that have a unit relative degree. The equations of the proposed TD are expressed as follows:

$$\dot{\tilde{e}}_1 = \tilde{e}_2 \quad (7)$$

$$\dot{\tilde{e}}_2 = -R^2\left(\frac{\tilde{e}_1 - \tilde{e}}{1 + |\tilde{e}_1 - \tilde{e}|}\right) - R\tilde{e}_2 \quad (8)$$

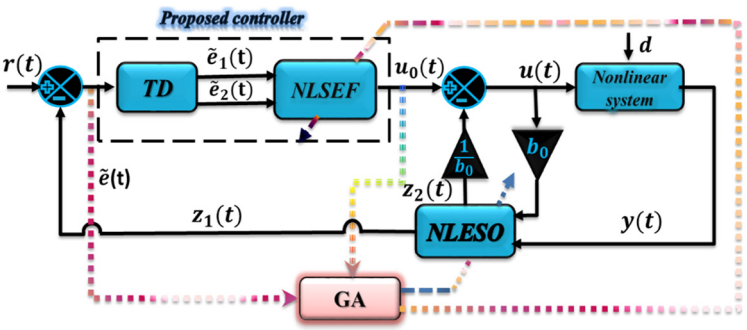

Fig. 2. The proposed relative degree one ($\rho = 1$) ADRC

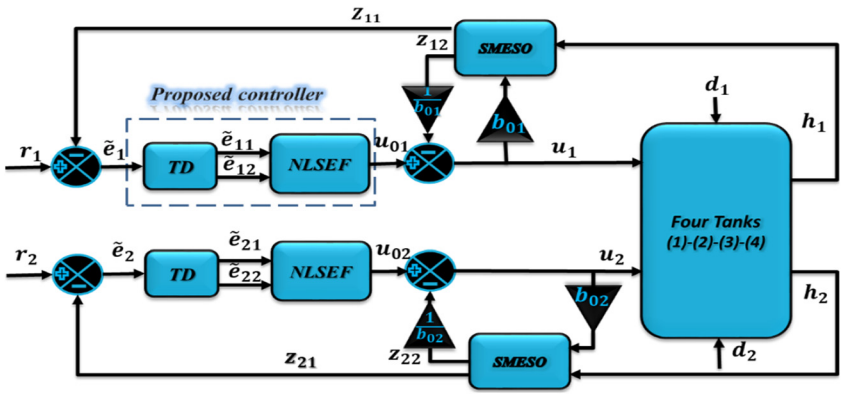

Fig. 3. Proposed ADRC with the nonlinear model of the four-tank system with unit relative degree ($\rho = 1$)

where $\tilde{e}_1$ is the tracking error and its equal to $\tilde{e}_1 = r - z_1$, $\tilde{e}_2$ is the derivative and $\tilde{e}$ is the input to the tracking differentiator and R is the parameter chosen to speed up or slow down the transient profile. In the next subsection, we will introduce the proposed controller and how we used the proposed TD with the nonlinear controller for systems with a unit relative degree.

3.2. Nonlinear TD-NLPID controller

NLPID is the modified version of the traditional PID controller. It is evolved to achieve fast process, high robustness, and stability and can handle the strong nonlinearity of the nonlinear systems, which the traditional PID controller fails to do. The main aim of the proposed controller is to treat the error function and its integration and derivative as a nonlinear function and thus satisfy the rule "small error large gain, large error small gain". The NLPID equations are expressed as follows,

$$u_{NLSEFi} = u_{i1} + u_{i2} + u_{integreator_i} \tag{9}$$

$$u_{i1} = \left(k_{11i} + \frac{k_{12i}}{1 + \exp(\mu_{i1}\tilde{e}_{i1}^2)}\right)|\tilde{e}_{i1}|^{\alpha_{i1}} sign(\tilde{e}_{i1}) \tag{10}$$

$$u_{i2} = \left(k_{21i} + \frac{k_{22i}}{1 + \exp(\mu_{i2}\dot{\tilde{e}}_{i1}^2)}\right)|\dot{\tilde{e}}_{i1}|^{\alpha_{i2}} sign(\dot{\tilde{e}}_{i1}) \tag{11}$$

$$u_{integrator_i} = \left(\frac{k_i}{1 + \exp\left(\mu_i \int \tilde{e}_{i1} dt^2\right)}\right)\left|\int \tilde{e}_{i1} dt\right|^{\alpha_i} sign\left(\int \tilde{e}_{i1}\, dt\right) \tag{12}$$

$$u_{0i} = \delta \tanh\left(\frac{u_{NLSEFi}}{\delta}\right) \tag{13}$$

where k_{11i}, k_{12i}, k_{21i}, k_{22i}, k_i, μ_{i1} and μ_{i2}, α_{i1}, α_{i2} are tuning design parameters and $\dot{\tilde{e}}_{i1} = \tilde{e}_{i2}$. Moreover, α_{i1} $\alpha_{i2} < 1$ to ensure the error functions $|\tilde{e}_{i1}|^{\alpha i1}$, $|\dot{\tilde{e}}_{i1}|^{\alpha i2}$ are sensitive to small error values [14, 20], and to satisfy the rule "*small error large gain, large error small gain*" [9]. The parameter δ is a positive coefficient that would make "tanh" function between the sector $[+\ \delta, -\delta]$ instead of $[+\infty, -\infty]$. In other words, "tanh" function will limit the control signal by δ which in turn cancels the high-frequency components, reduces the chattering in the control signal, and provides energy-saving [21, 22]. The new structure of the nonlinear controller that consists of an NLPID controller and a TD that is used to control the water level of the two lower tanks shows an excellent response and control. The main aim of the proposed controller for a system with a unit relative degree is that instead of using ordinary differentiation, we can use the benefits of the TD to get filtered error and its derivative and thus excluding higher values of the ordinary differentiation caused by noise. The stability analysis and design details of the NLPID controller can be referred to in [14].

3.3. Sliding mode extended state observer (SMESO)

The nonlinear ESO (NLESO) is more efficient and accurate than linear ESO (LESO) because the NLESO solves the problem of slow convergence and peaking phenomenon that exists in LESO [23, 24]. The SMESO estimates the total disturbance, system's state and converts the system into a chain of integrators. The SMESO is given by the following equations:

$$\dot{z}_{i1} = z_{i2} + b_{0i}u_i + \beta_{i1}k_i(e_{i1})e_{i1} \tag{14}$$

$$\dot{z}_{i2} = \beta_{i2}k_i(e_{i1})e_{i1} \tag{15}$$

$$k_i(e_{i1}) = k_{\alpha_i}|e_{i1}|^{\alpha_i - 1} + k_{\beta_i}|e_{i1}|^{\beta_i} \tag{16}$$

where $i = 1, 2$, $e_{i1} = h_i - z_{i1}$, e_i and z_{i1} are the estimated error and the estimated state of h_i respectively. $k_i(e_{i1})$ is a nonlinear function [13], α_i and β_i are positive tuning parameters that must be less than 1. k_{α_i} and k_{β_i} Are the nonlinear function gains and they are tuning parameters too. β_{i1} and β_{i2} Are the observer gain parameters and they are selected such that the characteristic polynomial $s^2 + \beta_{i1}s + \beta_{i2}$ is Hurwitz [11], and for simplicity $s^2 + \beta_{i1}s + \beta_{i2} = (s + \omega_{0i})^2$, where ω_{0i} is SMESO bandwidth and it would be the only tuning parameter. Thus, $\beta_{i1} = 2\omega_{0i}$ and $\beta_{i2} = \omega_{0i}^2$. The proposed ADRC with the nonlinear model of the four-tank system is shown in Fig. 3. Figure 3, represents the detailed form of Fig. 2. Four tanks

system has two inputs (u_1, u_2) and two output (h_1, h_2). The reference signal (r_1, r_2) represents the desired value of the water level in tank$_1$ and tank$_2$ respectively. As mentioned previously, for the system with a unit relative degree, there is no need for the TD. So, we can use it to generate the error $\tilde{e}_{11}$ and its derivative $\tilde{e}_{12}$ for the 1st subsystem and $\tilde{e}_{21}$, $\tilde{e}_{22}$ for the 2nd subsystem. Then, the estimated total disturbance will be canceled from the control signal of each subsystem (u_{01}, u_{02}) to generate the required control law, $u_i = (u_{0i} - z_{i2}/b_{0i})$, $i = 1, 2$. The state-space model and stability analysis of SMESO are presented in detail in [13].

4. CONVERGENCE OF THE SMESO

In this section, we will introduce the convergence of the Sliding Mode Extended State Observer (SMESO) using Lyapunov stability theorem.

For 1st subsystem, the error dynamics are stated in the following. Firstly, (1) is rewritten as:

$$\dot{h}_1 = f_1 + b_{01}d_1 + b_{01}u_1 \tag{17}$$

Let

$$h_{12} = f_1 + b_{01}d_1 \tag{18}$$

Now, sub. (18) In (17) yields,

$$\dot{h}_1 = h_{12} + b_{01}u_1 \tag{19}$$

Now differentiate (17) to get,

$$\dot{h}_{12} = \dot{f}_1 + b_{01}\dot{d}_1 \tag{20}$$

$$\begin{cases} \dot{h}_1 = h_{12} + b_{01}u_1 \\ \dot{h}_{12} = \dot{f}_1 + b_{01}\dot{d}_1 \end{cases} \tag{21}$$

where h_{12} is the generalized disturbance, f_1 is the system dynamics and parameter uncertainty and d_1 is the exogenous disturbance.

Now, for the $SMESO_1$ of the 1st channel, Eq. (14), (15) can be rewritten as

$$\begin{cases} \dot{z}_{11} = z_{12} + b_{01}u_1 + \beta_{11}k_1(e_{11})e_{11} \\ \dot{z}_{12} = \beta_{12}k_1(e_{11})e_{11} \end{cases} \tag{22}$$

From (5), and sub $k_c = 1$, h_1 can be found as

$$\begin{cases} h_1 = y/k_c \\ h_{12} = f_1 + b_{01}d_1 \end{cases} \tag{23}$$

The estimated error for subsystem1 can be written as

$$\begin{cases} e_{11} = h_1 - z_{11} \\ e_{12} = h_{12} - z_{12} \end{cases} \tag{24}$$

where e_{11} and e_{12} are the estimated errors, z_{11} is the estimated state of h_1, z_{12} is the estimated total disturbance of the 1st channel. Now differentiating (24) yields,

$$\begin{cases} \dot{e}_{11} = \dot{h}_1 - \dot{z}_{11} \\ \dot{e}_{12} = \dot{h}_{12} - \dot{z}_{12} \end{cases} \tag{25}$$

where $\dot{e}_{11}$ and $\dot{e}_{12}$ are the error dynamics for the 1st subsystem. Sub. (21), (22) in (25), yields,

$$\begin{cases} \dot{e}_{11} = -\beta_{11}k_1(e_{11})e_{11} + e_{12} \\ \dot{e}_{12} = -\beta_{12}k_1(e_{11})e_{11} + \dot{h}_{12} \end{cases} \tag{26}$$

In state-space form, (26) can be rewritten as

$$\begin{bmatrix} \dot{e}_{11} \\ \dot{e}_{12} \end{bmatrix} = \begin{bmatrix} -\beta_{11}k_1(e_{11}) & 1 \\ -\beta_{12}k_1(e_{11}) & 0 \end{bmatrix} \begin{bmatrix} e_{11} \\ e_{12} \end{bmatrix} + \begin{bmatrix} 0 \\ 1 \end{bmatrix} \dot{h}_{12}$$

So, the general form of the error dynamics is

$$\dot{e}_i = A_i e_i + \dot{h}_{i2} \tag{27}$$

where i refers to the subsystem number which is either 1 or 2, $A_i = \begin{bmatrix} -\beta_{i1}k_i(e_{i1}) & 1 \\ -\beta_{i2}k_i(e_{i1}) & 0 \end{bmatrix}$, $\dot{e}_i = \begin{bmatrix} \dot{e}_{i1} \\ \dot{e}_{i2} \end{bmatrix}$ and $e_i = \begin{bmatrix} e_{i1} \\ e_{i2} \end{bmatrix}$. Now to check that whether the estimated error converges to zero as $t \to \infty$, i.e., the SMESO is asymptotically stable. To achieve that, Lyapunov stability is used [25]. Let us choose the Lyapunov function as $V_{SMESO_i} = \frac{1}{2}e_i^T e_i$. Then,

$$\begin{aligned} \dot{V}_{SMESO_i} &= e_i^T \dot{e}_i \dot{V}_{SMESO_i} \\ &= \begin{bmatrix} e_{i1} & e_{i2} \end{bmatrix} \begin{bmatrix} -\beta_{i1}k_i(e_{i1}) & 1 \\ -\beta_{i2}k_i(e_{i1}) & 0 \end{bmatrix} \begin{bmatrix} e_{i1} \\ e_{i2} \end{bmatrix} + \dot{h}_{i2} \end{aligned}$$

Assume that $\dot{h}_{i2}$ converges to zero as $t \to \infty$ (which is the case for constant exogenous disturbances) [13], then,

$$\dot{V}_{SMESO_i} = \begin{bmatrix} e_{i1} & e_{i2} \end{bmatrix} \begin{bmatrix} -\beta_{i1}k_i(e_{i1}) & 1 \\ -\beta_{i2}k_i(e_{i1}) & 0 \end{bmatrix} \begin{bmatrix} e_{i1} \\ e_{i2} \end{bmatrix}$$

The quadric form $\dot{V}_{SMESO_i} = e_i^T Q_i \dot{e}_i$ is asymptotically stable if Q_i is a negative definite matrix. Then, according to [25], the system is asymptotically stable when the following conditions are satisfied,

1. V_{SMESO_i} is positive definite, $V_{SMESO_i}(e_i) > 0 \; for \; e_i \neq 0$, $i = 1, 2$.
2. $\dot{V}_{SMESO_i}(e_i) < 0 \; for \; e_i \neq 0$, $i = 1, 2$.

Now to check the negative definiteness of Q_i, Routh stability criteria can be used to find the stability limits of matrix Q_i. Firstly, compute the characteristic equation for matrix Q_i,

$$|\lambda \mathrm{I} - Q_i| = 0, \begin{vmatrix} \lambda + \beta_{i1}k_i(e_{i1}) & -1 \\ \beta_{i2}k_i(e_{i1}) & \lambda \end{vmatrix} = 0$$

$$\lambda^2 + \beta_{i1}k_i(e_{i1})\lambda + \beta_{i2}k_i(e_{i1}) = 0$$

where $i = 1, 2$. Then from Routh stability criteria, one gets,

1	$\boldsymbol{\beta_{i2}k_i(e_{i1})}$
$\boldsymbol{\beta_{i1}k_i(e_{i1})}$	0
$\frac{\beta_{i1}\beta_{i2}k_i(e_{i1})^2 - 0}{\beta_{i1}k_i(e_{i1})} = \boldsymbol{\beta_{i2}k_i(e_{i1})}$	0

$\beta_{i1}k_i(e_{i1}) > 0$, $k_i(e_{i1}) > 0$. Then Q_i is negative definite if the nonlinear gain $k_i(e_{i1})$ satisfies $k_i(e_{i1}) > 0$. We conclude that the SMESO is asymptotically stable.

Table 1. Sample parameters of the Four-tank system

Parameter	Value	Unit
h_1	16	cm
h_2	13	cm
h_3	9.5	cm
h_4	6	cm
γ_1	0.7	$unitless$
γ_2	0.6	$unitless$
k_1	3.33	$cm^3/volt.sec$
k_2	3.35	$cm^3/volt.sec$
a_1	0.071	cm^2
a_2	0.056	cm^2
a_3	0.071	cm^2
a_4	0.056	cm^2
A_1	28	cm^2
A_2	32	cm^2
A_3	28	cm^2
A_4	32	cm^2
k_c	1	$volt/cm$
g	981	cm/sec^2

5. SIMULATION RESULTS AND DISCUSSION

5.1. Simulation results

The proposed ADRC for the Four-tank nonlinear model is designed and simulated using Matlab/Simulink. The parameters of the Four-tank model are shown in Table 1. The simulations include comparing the proposed scheme with four different schemes. The Genetic Algorithm is used in the paper as an optimization technique [26, 27], and [28], to tune the parameters of the NLPID controller, SMESO, and TD of all schemes including the proposed one. In addition, to measure the performance of the entire system, a useful multi-Objective Performance Index (OPI) has been used in this work. It measures the effectiveness of the proposed scheme and it is expressed as follows

$$OPI = w_1{*}OPI_1 + w_2{*}OPI_2 \tag{28}$$

where OPI_1 and OPI_2 represent the objective performance index for the first and second subsystems respectively, w_1 and w_2 are weighting factors. To treat the two subsystems equally likely, w_1 and w_2 are set to 0.5. Both OPI_1 and OPI_2 are expressed as

$$\begin{cases} OPI_1 = W_1{*}\dfrac{ITAE_1}{N_{11}} + W_2{*}\dfrac{UABS_1}{N_{12}} + W_3{*}\dfrac{USEQ_1}{N_{13}} \\ OPI_2 = W_1{*}\dfrac{ITAE_2}{N_{21}} + W_2{*}\dfrac{UABS_2}{N_{22}} + W_3{*}\dfrac{USEQ_2}{N_{23}} \end{cases} \tag{29}$$

where W_1, W_2 and W_3 are the weighting factors that satisfy $W_1 + W_2 + W_3 = 1$. According to that, they are set to $W_1 = 0.4$, $W_2 = 0.2$ and $W_3 = 0.4$. $N_{11}, N_{12}, N_{13}, N_{21}, N_{22}$ and N_{23} are the nominal values of the individual objective functions, which are included in the OPI to ensure that the individual objectives have comparable values and are treated equally likely by the tuning algorithm. Thus, their values are set to $N_{11} = 1.814362$, $N_{12} = 4389.201$, $N_{13} = 305.59$, $N_{21} = 1.77746$, $N_{22} = 4332.233$, and $N_{23} = 285.2937$. Table 2 shows the description and mathematical representation of the performance indices.

The Five schemes that were simulated in this work are listed as follows,

1. Scheme$_1$: (LADRC). Linear State Error Feedback (LSEF) [9] + LESO.

   The LESO is expressed as follows,

$$\begin{cases} \dot{z}_{i1} = z_{i2} + b_{0i}u_i + \beta_{i1}(e_{i1}) \\ \dot{z}_{i2} = \beta_{i2}(e_{i1}) \end{cases} \tag{30}$$

   The parameters of Eq. (30) are already previously in this work.

2. Scheme$_2$: (NLADRC). Nonlinear State Error Feedback (NLSEF) [9] + LESO of Eq. (30).

   The NLSEF is given by

$$\begin{cases} fal(\tilde{e}_{i1},\, \alpha_{1i},\, \delta_{1i}) = \begin{cases} \tilde{e}_{i1}/\left(\delta_{i1}^{1-\alpha_{i1}}\right),\ x \le \delta_{i1} \\ |\tilde{e}_{i1}|^{\alpha_{i1}} sign(\tilde{e}_{i1}),\ x > \delta_{i1} \end{cases} \\ fal(\tilde{e}_{i2},\, \alpha_{i2},\, \delta_{i2}) = \begin{cases} \tilde{e}_{i2}/\left(\delta_{i2}^{1-\alpha_{i2}}\right),\ x \le \delta_{i2} \\ |\tilde{e}_{i2}|^{\alpha_{i2}} sign(\tilde{e}_{i2}),\ x > \delta_{i2} \end{cases} \end{cases} \tag{31}$$

$$\begin{cases} \begin{cases} u_{01} = fal(\tilde{e}_{11},\, \alpha_{11},\, \delta_{11}) + fal(\tilde{e}_{12}, \alpha_{12},\, \delta_{12}) \\ u_{02} = fal(\tilde{e}_{21},\, \alpha_{21},\, \delta_{21}) + fal(\tilde{e}_{22},\, \alpha_{22},\, \delta_{22}) \end{cases} \\ \begin{cases} u_1 = (u_{01} - z_{12})/b_{01} \\ u_2 = (u_{02} - z_{22})/b_{02} \end{cases} \end{cases} \tag{32}$$

   where $i = 1, 2$, $\tilde{e}_{i1} = r_i - z_{i1}$, e_{i2} are the tracking error and its derivative respectively, $\alpha_{11}, \alpha_{12}, \alpha_{21}, \alpha_{22}, \delta_{11}, \delta_{12}, \delta_{21}$ and δ_{22} are positive tuning parameters.

3. Scheme$_3$: TD of Eq. (7–8) + NLSEF of Eq. (31), (32) + LESO of Eq. (30).
4. Scheme$_4$: SMESO [13] + nonlinear proportional gain (NLP) of Eq. (10).
5. Proposed scheme: SMESO of Eq. (14)–(16) + NLPID of Eq. (10)–(13) + TD Eq. (7)–(8).

The simulated results for each scheme are given next. The tuned parameters of both the controller and the observer of each scheme (1, 2, 3, and 4) are given in Tables 3–7.

Table 2. Description and mathematical representation of performance

PI	Description	Mathematical representation
ITAE	Integral time absolute error	$\int_0^{tf} t\|e(t)\|dt$
UABS	Integral absolute of the control signal	$\int_0^{tf} \|u(t)\|dt$
USEQ	Integral square of the control signal	$\int_0^{tf} u(t)^2 dt$

Table 3. Parameters of scheme $_1$

Parameter	Value	Parameter	Value
k_{p1}	18.6300	k_{d2}	3.0500
k_{i1}	0.0002	β_{11}	86.2600
k_{d1}	2.5300	β_{12}	1860.2
k_{p2}	26.6550	β_{21}	31.8200
k_{i2}	0.0024	β_{22}	253.1281

Table 4. Parameters of scheme$_2$

Parameter	Value	Parameter	Value
α_1	0.7763	β_{11}	298.6900
δ_1	0.0140	β_{12}	2230.4
α_2	0.4167	β_{21}	349.0100
δ_2	1.8958	β_{22}	2993.1

Table 5. Parameters of scheme$_3$

Parameter	Value	Parameter	Value
α_{11}	0.6190	δ_{22}	0.7441
δ_{11}	0.0238	R	300
α_{12}	0.7115	β_{11}	326.1200
δ_{12}	0.9276	β_{12}	2658.9
α_{21}	0.5813	β_{21}	270.2800
δ_{21}	0.0814	β_{22}	1826.3
α_{22}	0.9905	-	-

Table 6. Parameters of scheme$_4$

Parameter	Value	Parameter	Value
k_{111}	6.2650	k_{212}	7.0400
k_{121}	1.4124	k_{222}	0.0142
μ_{11}	8.5790	μ_{22}	5.6130
α_{11}	0.6812	α_{22}	0.6625

Table 7. Parameters of scheme$_4$

Parameter	Value	Parameter	Value
β_{11}	266.4000	k_{β_1}	0.6713
β_{12}	1774.2	β_1	0.2221
β_{21}	327.6800	k_{α_2}	0.8579
β_{22}	2684.4	α_2	0.6265
k_{α_1}	0.3675	k_{β_2}	0.6812
α_1	0.9733	β_2	0.7062

Table 9. Parameters values of the proposed scheme (SMESO part)

Parameter	Value	Parameter	Value
β_{11}	294.8600	k_{β_1}	0.7648
β_{12}	2173.6	β_1	0.8946
β_{21}	218.1000	k_{α_2}	0.5705
β_{22}	1189.2	α_2	0.7124
k_{α_1}	0.1095	k_{β_2}	0.5773
α_1	0.6964	β_2	0.7942

The values of the parameter for the proposed scheme are listed in Tables 8 and 9.

The water level of tank$_1$ and tank$_2$ are shown in Figs 4–5. The results show that the output response of the proposed scheme is faster, smoother, and without overshooting as compared to that of the other schemes. It takes about less than 2s to reach the steady-state (desired value), while a longer settling time is clearly shown in the output response of the other schemes. Figures 6 and 7 show the output response in the existence of the disturbance for the 1st subsystem at t = 40s and the 2nd subsystem at t = 60s. The results show that scheme$_1$, scheme$_2$ scheme$_3$, and scheme$_4$ when applying disturbance for 1st subsystem at t = 40s exhibit an output response with an undershoot which reaches nearly 0.1265%, 0.375%, 0.1875%, 0.125% respectively of the steady-state value and last about 1.2 s for scheme$_1$, 2.1s for scheme$_2$, 1s for scheme$_3$ and 0.5s for scheme$_4$ until the output response reaches its steady state. The same for 2nd subsystem, at t = 60s the, output response exhibits an undershoot which reaches nearly 0.307%, 0.315%, 0.305%, 0.153% of its steady-state value for scheme$_1$, scheme$_2$ scheme$_3$, and scheme$_4$ respectively and last about 1.9 s for scheme$_1$, 1.92s for scheme$_2$, 1.5s for scheme$_3$ and 0.5s for scheme$_4$ until it reaches its steady-state, while our proposed scheme rejects the disturbance very quickly.

Figures 8 and 9 show the control signal for the 1st subsystem and the 2nd subsystem. The proposed scheme shows chattering free, whilescheme$_2$ shows chattering in the control signal. This proves that the proposed scheme is better than other schemes.

To observe the effect of the system parameter uncertainty on the four tanks model, the value of the outlet hole a_1 is varied by ($\Delta_{a_1} = \mp 2\%$). Figure 10 show the response of the water level of tank$_1$ while applying the uncertainties. (a) with uncertainty ($\Delta_{a_1} = +2\%$). (b) with uncertainty ($\Delta_{a_1} = -2\%$). It is observed that the proposed scheme can

Table 8. The parameters of the proposed scheme (NLSEF part)

Parameter	Value	Parameter	Value	Parameter	Value
k_{111}	10.6800	k_1	0.7124	k_{222}	2.1384
k_{121}	2.3826	μ_1	7.9420	μ_{22}	3.5100
μ_{11}	5.7050	α_1	0.5705	α_{22}	0.7073
α_{11}	0.5773	k_{211}	10.5285	k_2	0.5773
k_{112}	2.3715	k_{221}	1.1070	μ_2	1.5810
k_{122}	0.8844	μ_{21}	3.4640	α_2	0.2948
μ_{12}	0.2240	α_{21}	0.6184	δ	37.4430
α_{12}	0.5189	k_{212}	2.5620	R	100

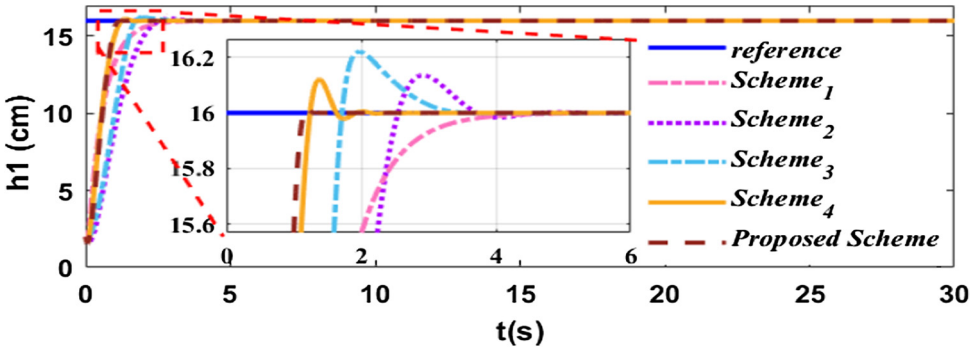

Fig. 4. Water level in tank$_1$

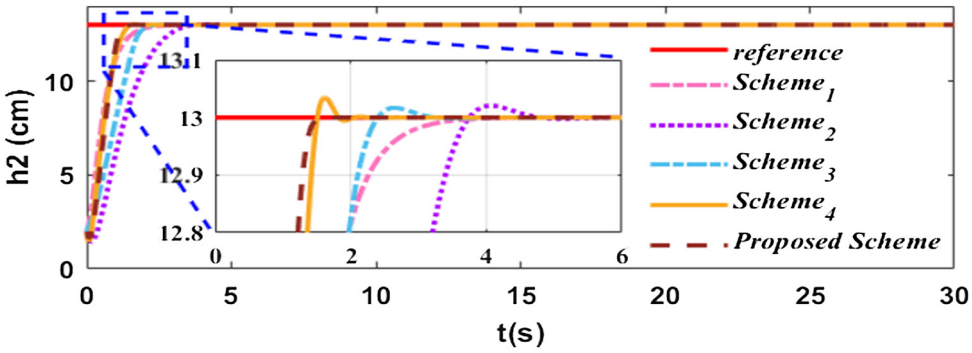

Fig. 5. Water level in tank$_2$

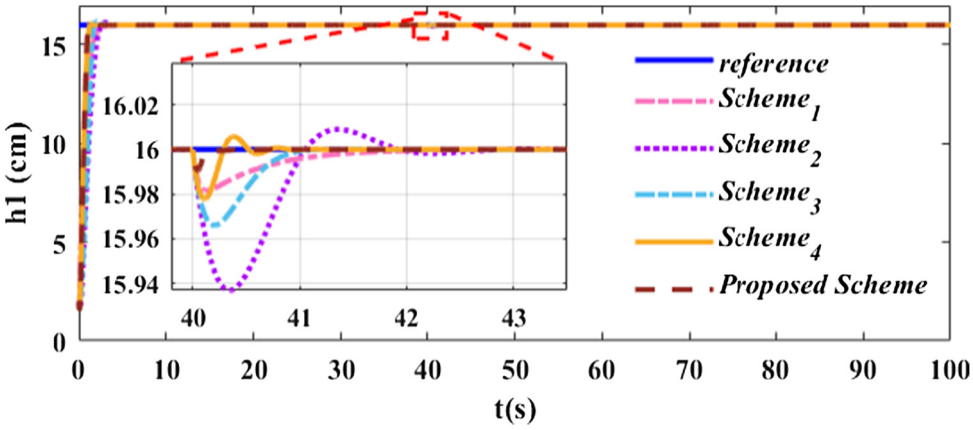

Fig. 6. A disturbance is applied for 1st subsystem at $t = 40$s

handle the uncertainties with high performance, which shows the effectiveness of the SMESO.

5.2. Discussions

From the presented results, it is clearly shown that with the proposed scheme, the water level arrives at its steady-state (desired value) in a shorter time as compared to other schemes used in the comparison and without overshooting or undershooting. Even when a disturbance is applied to the system (at $t = 40$ disturbance applied to the 1st subsystem and at $t = 60$ disturbance applied to the 2nd subsystem), the disturbance does not affect the system's output due to the excellent estimation of the SMESO to the total disturbance which is canceled from the input channel via the SMESO. Moreover, when the parameter uncertainty of $\Delta_{a_1} = \mp 2\%$ is applied to the system, the variation in the outlet hole $\boldsymbol{a}_1$ does not affect the system output. The inclusion of the SMESO in the feedback loop reduced the peaking phenomenon that was visible when using the LESO (e.g., scheme$_1$, scheme$_2$, scheme$_3$). Moreover, the control signal of the proposed scheme shows a reduction in chattering due to the adoption of the new nonlinear controller as compared to the other schemes. The new NLPID controller is nonlinear and satisfies the rule "*small error large gain, large error, small gain*" which works by producing a chattering-free control signal. Table 10 shows the simulated results of the performance

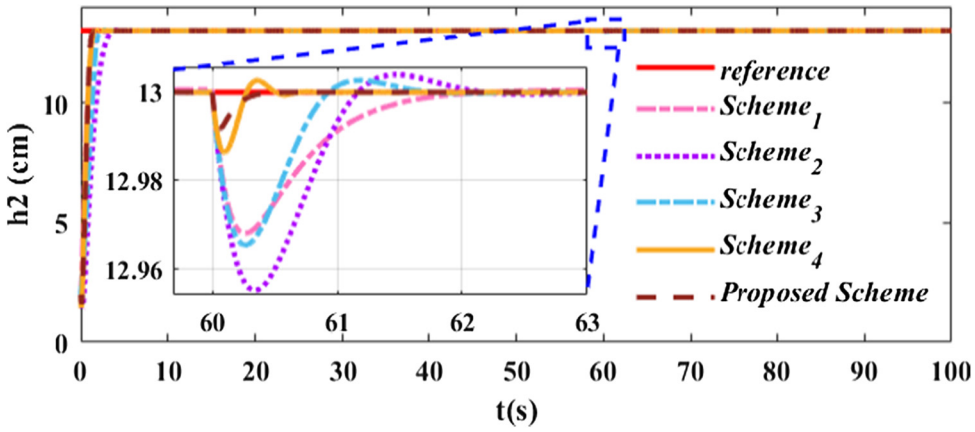

Fig. 7. A disturbance is applied for 2nd subsystem at $t = 60$s

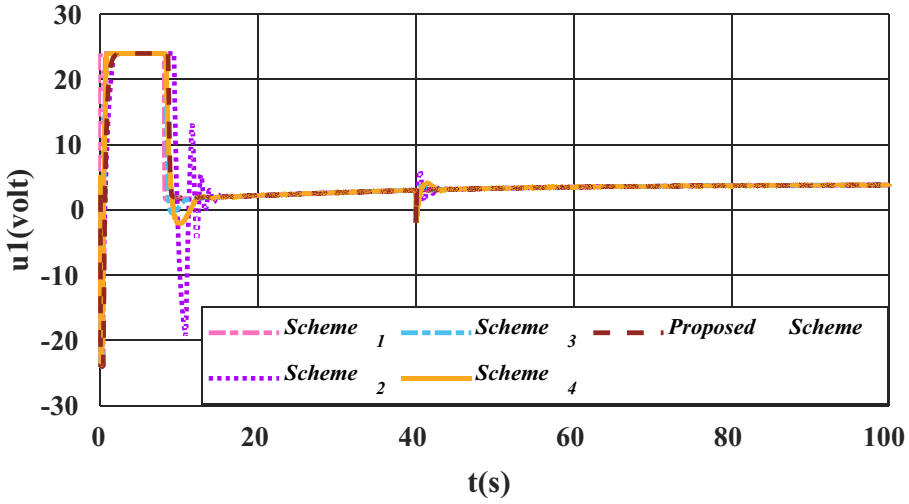

Fig. 8. The control signal for the 1st subsystem

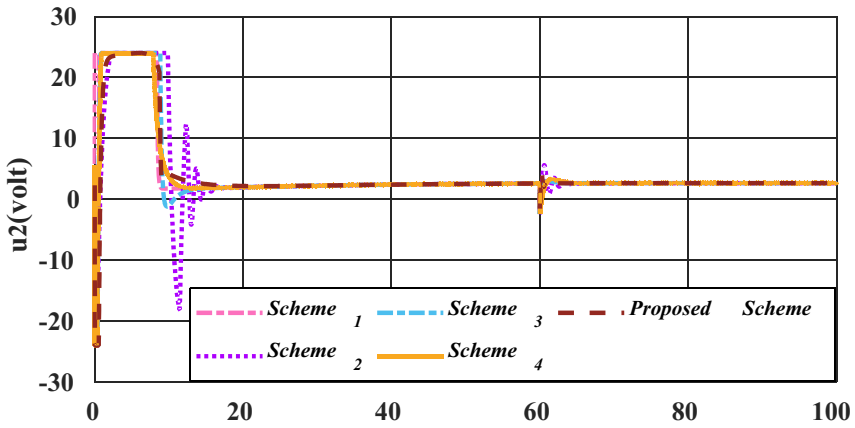

Fig. 9. The control signal for the 2nd subsystem

indices after GA tuning for all the schemes that are applied in this work including the proposed one. Table 11 lists the complete abbreviations used in this paper. As shown in Table 10, the proposed scheme shows an improvement for the transient response, in other words, $ITAE_1$ and $ITAE_2$ are reduced by 50.4% and 40.31% respectively as compared to the other schemes. Finally, the proposed scheme achieves the best OPI, $ITAE_1$ and $ITAE_2$ among all the other schemes.

Now we will show the effectiveness of our proposed method compared with other methods as follows:

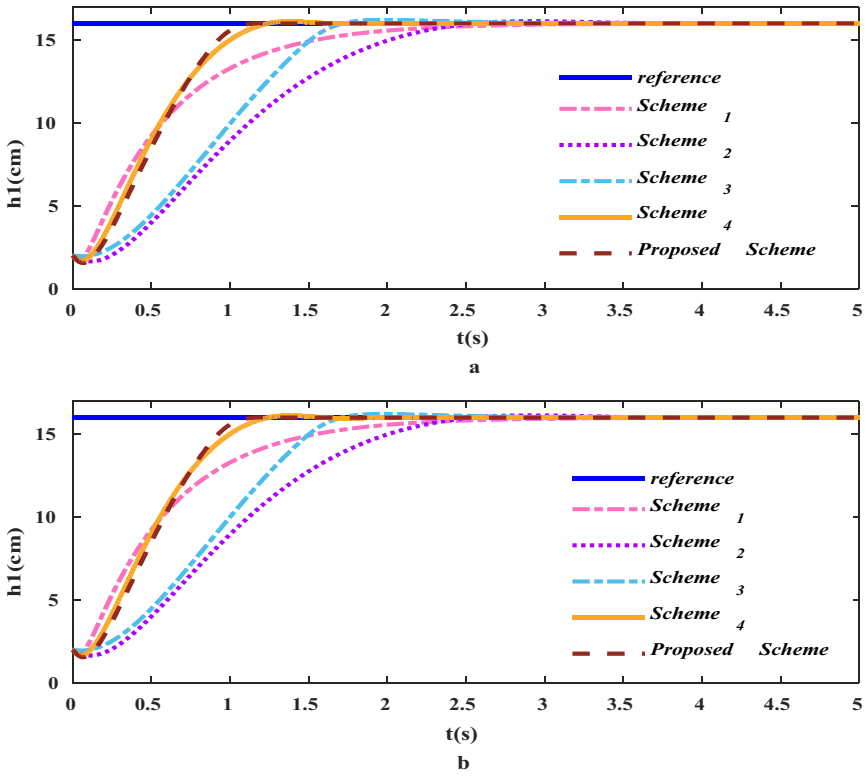

Fig. 10. The water level in tank $_1$ with uncertainty in the outlet hole a_1

Table 10. Simulation Results for the Four Tanks System

Schemes/PI	scheme $_1$	scheme $_2$	scheme $_3$	scheme $_4$	Proposed scheme
$ITAE_1$	5.044853	10.731810	7.361344	2.609788	2.501022
$ITAE_2$	7.514269	13.463353	6.396127	2.684229	2.642392
$UABS_1$	13115.098625	976.413223	649.113747	2518.480536	2480.090176
$UABS_2$	16124.0015950	1021.529276	618.459631	2695.503633	2684.961943
$USEQ_1$	16194.336535	54.015678	27.778464	678.346693	666.768796
$USEQ_2$	20840.561939	46.700165	61.123995	658.756634	705.609611
OPI	23.21906907	2.481163	1.688843	1.578022	1.537139

1. In [6], Figs 2 and 3 shows that the water level reaches the steady-state (desired value) in about 13 s, while in our proposed scheme, it is observed that the water level reaches the desired value in less than 2 s with smooth fast response. Moreover, when the disturbance is applied, the system of [6], Figs 8 and 9 shows a noticeable overshoot and undershoot. This proves the robustness of our proposed scheme.
2. In [12], Fig. 4 (a, b) shows that the water level for both $tank_1$ and $tank_2$ rises with rising time $t_r = 25$ s and $t_r = 15$ s for ADRC and LADRC respectively. While the water level using our proposed scheme rises faster with rising time $t_r = 0.667944$ s and $t_r = 0.742405$ s for $tank_1$ and $tank_2$ respectively without any noticeable oscillations. In addition, the system of [12] under the disturbance recovered to the desired value after 10 and 1s for ADRC and LADRC respectively, while our proposed method rejects the disturbance very quickly.
3. In [15], the linearized model of the four tanks system is used. Figure 4 shows the response of the two lower tanks ($tank_1$ and $tank_2$) that rises with rising time $t_r = 1.3$ s. When the disturbance is applied, the response is not smooth enough. On the other hand, our proposed scheme shows a fast, smooth response with rising time $t_r = 0.667944$ s and $t_r = 0.742405$ s for $tank_1$ and $tank_2$ respectively.
4. In [16], Table 6 shows the performance indices for both $tank_1$ and $tank_2$. It is observed that the system of [16] has $ITAE_1 = 8.0567*10^7$ and $ITAE_2 = 2.7820*10^8$ for ASMC controller. While our proposed scheme has $ITAE_1 = 2.501022$ and $ITAE_2 = 2.642392$ for $tank_1$ and $tank_2$ respectively. This proves the effectiveness of our scheme.
5. In [17], Fig. 10 shows a noticeable overshoot in the response of $tank_2$, while our proposed scheme shows a smooth response with fast convergence. In this research, the effect of disturbance and parameter uncertainties have not been taken into consideration.

Table 11. List of abbreviations used in this paper

Abbreviation	Definition
TD	Tacking Differentiator
OPI	Objective Performance Index
ITAE	Integral Time Absolute Error
UABS	Integral Absolute of the control signal (IAU)
USEQ	Integral Square of the control signal (ISU)
MIMO	Multi-Input Multi-Output system
ADRC	Active Disturbance Rejection Control
LESO	Linear Extended State Observer
LPID	Linear proportional-Integral- Derivative
LSEF	Linear State Error Feedback
NLESO	Nonlinear Extended State Observer
SMESO	Sliding Mode Extended State Observer
NLSEF	Nonlinear State Error Feedback
NLPID	Nonlinear Proportional -Integral-Derivative
$_{hj}$	The water level of tank $_{j}$
γ_1, γ_2	Ration of the flow in the valves
$_{k1}$, k_2	Pump proportionality constant
$_{aj}$	The cross-section area of the outlet hole of tank $_{j}$
A_j	The cross-section area of the tank $_{j}$
k_c	The calibrated constant
g	Gravity constant
ASMC	Adaptive Sliding Mode Controller
APPC	Adaptive Pole Placement Controller

6. CONCLUSIONS

This work proposes a control scheme, i.e., (TD+NLPID) that is applied to the nonlinear model of the four-tank system which achieves the following:

- It produces fast-tracking, makes the system less sensitive to noise and reduces the chattering that is produced by other schemes in the control signal, which subsequently increases energy consumption.
- The proposed control scheme TD+NLPID reduces the noise in the closed-loop system, which is amplified when using ordinary derivatives in traditional PID control or LSEF control. The SMESO is not just cancelling the disturbance and estimate system's states, but, also reduces the peaking, a natural phenomenon in the LESO-based control schemes. This is due to the adoption of a nonlinear error function that is used in the design with asymptotic convergence.
- The proposed TD-NLPID control scheme solves the main aims of this paper with excellent results and performance for a system that has a unit relative degree, strong nonlinearities, MIMO coupling interacting, multivariable zeros that make the system operate in two modes (minimum and non-minimum phase).
- An extension to the current work includes the H/W implementation of the proposed TD-NLPID control scheme on a real four-tank system platform using one of the recent stand-alone computing systems like Arduino or Raspberry PI. Furthermore, applying other control techniques on the four-tank system and comparing the obtained results with that of this work [29–35].

REFERENCE

[1] K. H. Johansson, "The Quadruple-Tank Process-A multivariable laboratory process with an adjustable zero," *IEEE Control Syst. Technol*, vol. 8, no. 3, pp. 456–65, 2000. Available: https://doi.org/10.1109/87.845876.

[2] K. H. Johansson, A. Horch, O. Wijk, and A. Hansson, "Teaching multivariable control using the quadruple-tank process," in *Proceedings of the 38th IEEE Conference on Decision and Control (Cat. No.99CH36304)*, Phoenix, AZ, USA, (1), 1999, pp. 807–12. https://doi.org/10.1109/CDC.1999.832889.

[3] K. H. Johansson and J. L. R. Nunes, "A multivariable laboratory process with an adjustable zero," in *Proceedings of the 1998 American Control Conference. ACC (IEEE Cat. No.98CH36207)*, Philadelphia, Pennsylvania, (4), 1998, pp. 2045–9. https://doi.org/10.1109/ACC.1998.702986.

[4] C. Ramadevi and V. Vijayan, "Design of decoupled PI controller for quadruple tank system," *Int. J. Sci. Res. (IJSR)*, vol. 3, no. 5, pp. 318–23, 2014.

[5] S. N. Deepa and A. Raj, "Modeling and implementation of various controllers used for quadruple- tank," in *International Conference on Circuit, Power and Computing Technologies (ICCPCT)*, Nagercoil, India, 2016, pp. 1–5. https://doi.org/10.1109/ICCPCT.2016.7530245.

[6] V. Chaudhari, B. Tamhane, and S Kurode, "Robust liquid level control of quadruple tank system-second order sliding mode," *IFAC Pap. On-Line*, vol. 53, no. 1, pp. 7–12, 2020. Available: https://doi.org/10.1016/j.ifacol.2020.06.002.

[7] K. Divya, M. Nagarajapandian, and T. Anitha, "Design and implementation of controllers for quadruple tank system," *Int. J. Adv. Res. Edu. Technol. (IJARET)*, vol. 4, no. 2, pp. 158–65, 2017.

[8] A. Abdullah and M. Zribi, "Control schemes for a quadruple tank process," *Int. J. Comput. Commun. Control*, vol. 7, no. 4, pp. 594–604, 2012.

[9] J. Han, "From PID to active disturbance rejection control," *IEEE Trans. Ind. Elect.*, vol. 56, no. 3, pp. 900–6, 2009. Available: https://doi.org/10.1109/TIE.2008.2011621.

[10] J. Li, X. Qi, Y. Xia, and Z. Gao, "On asymptotic stability for nonlinear ADRC based control system with application to the ball-beam problem," *2016 American Control Conference (ACC)*, pp. 4725–30, 2016. Available: https://doi.org/10.1109/ACC.2016.7526100.

[11] Z. Gao, "Scaling and bandwidth-parameterization based controller tuning," in *Proceedings of the 2003 American Control Conference*, 2003, pp. 4989–96. https://doi.org/10.1109/ACC.2003.1242516.

[12] X. Meng, H. Yu, J. Zhang, T. Xu, and H. Wu, "Liquid level control of four-tank system based on active disturbance rejection technology," *Measurement*, no. 175, 2021. Available: https://doi.org/10.1016/j.measurement.2021.109146.

[13] I. K. Ibraheem and W. R. Abdul-Adheem, "Improved sliding mode nonlinear extended state observer-based active disturbance rejection control for uncertain systems with unknown total disturbance," *Int. J. Adv. Comput. Sci. Appl. (IJACSA)*, vol. 7, no. 12,

pp. 80–93, 2016. Available: https://doi.org/10.14569/IJACSA.2016.071211.

[14] I. K. Ibraheem and W. R. Abdul-Adheem, "From PID to nonlinear state error feedback controller," *Int. J. Adv. Comput. Sci. Appl. (IJACSA)*, vol. 8, no. 1, pp. 312–22, 2017. Available: https://doi.org/10.14569/IJACSA.2017.080140.

[15] B. Ashok Kumar, R. Jeyabharathi, S. Surendhar, S. Senthilrani and S. Gayathri, "Control of four tank system using model predictive controller," in *2019 IEEE International Conference on System, Computation, Automation and Networking (ICSCAN)*, 2019, pp. 1–5. https://doi.org/10.1109/ICSCAN.2019.8878700.

[16] A. Osman, T. Kara, and M. Arıcı, "Robust adaptive control of a quadruple tank process with sliding mode and pole placement control strategies," *IETE Journal of Research*, pp. 1–14, 2021. https://doi.org/10.1080/03772063.2021.1892537.

[17] F. D. J. Sorcia-Vázquez, C. D. Garcia-Blteran, G. Valencia-Palomo, J. A. Brizuela-Mendoza, and J. Y. Rumbo-Morales, "Decentralized robust tube-based model predictive control: application to a four-tank system," *Revista Mexicana de Ingeniería Química*, vol. 19, no. 3, pp. 1135–51, 2021. Available: https://doi.org/10.24275/rmiq/Sim778.

[18] K. Kiš, M. Klaučo and A. Mészáros, "Neural network controllers in chemical technologies," in *2020 IEEE 15th International Conference of System of Systems Engineering (SoSE)*, 2020, pp. 397–402. https://doi.org/10.1109/SoSE50414.2020.9130425.

[19] I. K. Ibraheem and W. R. Adul-Adheem, "A novel second-order nonlinear differentiator with application to active disturbance rejection control," in *2018 1st International Scientific Conference of Engineering Sciences - 3rd Scientific Conference of Engineering Science (ISCES)*, 2018, pp. 68–73. https://doi.org/10.1109/ISCES.2018.8340530.

[20] I. K. Ibraheem, "*Anti-Disturbance Compensator Design for Unmanned Aerial Vehicle*," *jcoeng*, vol. 26, no. 1, pp. 86–103, 2019. https://doi.org/10.31026/j.eng.2020.01.08.

[21] I. K. Ibraheem and W. R. Abdul-Adheem, "An improved active disturbance rejection control for a differential drive mobile robot with mismatched disturbances and uncertainties", arXiv e-print, arXiv:1805.12170, 2018.

[22] A. A. Najm and I. K. Ibraheem, "Nonlinear PID controller design for a 6-DOF UAV quadrotor system," *Engineering Science and Technology, an International Journal*, vol. 22, no. 4, pp. 1087–97, 2019. Available: https://doi.org/10.1016/j.jestch.2019.02.005.

[23] A. J. Humaidi and I. K. Ibraheem, "Speed control of permanent magnet DC motor with friction and measurement noise using novel nonlinear extended state observer-based anti-disturbance control," *Energies*, vol. 12, no. 9, p. 1651, 2019. Available: https://doi.org/10.3390/en12091651.

[24] B. Z. Guo and Z. H. Wu, "Output tracking for a class of nonlinear systems with mismatched uncertainties by active disturbance rejection control," *Systems & Control Letters*, vol. 100, pp. 21–31, 2017. Available: https://doi.org/10.1016/j.sysconle.2016.12.002.

[25] K. H. Khalil (2015). *Nonlinear control, global edition*, Pearson Education, 2015.

[26] A. J. Humaidi, I. K. Ibraheem, and A. R. Ajel, "A novel adaptive LMS algorithm with genetic search capabilities for system identification of adaptive FIR and IIR filters," *Information*, vol. 10, no. 5, p. 176, 2019. Available: https://doi.org/10.3390/info10050176.

[27] M. A. Joodi, I. K. Ibraheem, and F. M. Tuaimah, "Power transmission system midpoint voltage fixation using SVC with genetic tuned simple PID controller," *International Journal of Engineering & Technology*, vol. 7, no. 4, pp. 5438–43, 2018. https://doi.org/10.14419/ijet.v7i4.24799.

[28] A. A. Najm, I. K. Ibraheem, A. T. Azar, and A. J. Humaidi, "Genetic optimization-based consensus control of multi-agent 6-DoF UAV system," *Sensors*, vol. 20, no. 12, p. 3576, 2020. Available: https://doi.org/10.3390/s20123576.

[29] A. V. Okpanachi (2010), *Developing Advanced Control Strategies for a 4-Tank Laboratory process*", Master Thesis, Faculty of Technology Telemark University College.

[30] V. Chaudhari, B. Tamhane, and S. Kurode, "Robust liquid level control of quadruple tank system - second order sliding mode approach," *IFAC-PapersOnLine*, vol. 53, no. 1, pp. 7–12, 2020. Available: https://doi.org/10.1016/j.ifacol.2020.06.002.

[31] I. K. Ibraheem, "On the frequency domain solution of the speed governor design of non-minimum phase hydro power plant," *Mediterr J Meas Control*, vol. 8, no. 3, pp. 422–9, 2012.

[32] I. A. Mohammed, R. A. Maher, and I. K. Ibraheem, "Robust controller design for load frequency control in power systems using state-space approach," *Journal of Engineering*, vol. 17, no. 3, pp. 265–78, 2011.

[33] F. M. Tuaimah and I. K. Ibraheem, "Robust h∞ controller design for hydro turbines governor," 2nd Regional Baghdad, Iraq: Conf. for Eng.Sciences/ College of Eng./ Al-Nahrain University, 2010, pp. 1–9.

[34] R. A. Maher, I. A. Mohammed, and I. K. Ibraheem, "Polynomial based H∞ robust governor for load frequency control in steam turbine power systems," *International Journal of Electrical Power & Energy Systems*, vol. 57, pp. 311–7, 2014. Available: https://doi.org/10.1016/j.ijepes.2013.12.010.

[35] I. K. Ibraheem, "A digital-based optimal AVR design of synchronous generator exciter using LQR technique," *Al-Khwarizmi Engineering Journal*, vol. 7, no. 1, pp. 82–94, 2011.